Title
Sclerostin expression in skeletal sarcomas

Authors
Shen, Jia
Meyers, Carolyn A
Shrestha, Swati
et al.

Publication Date
2016-12-01

DOI
10.1016/j.humpath.2016.07.016

Peer reviewed

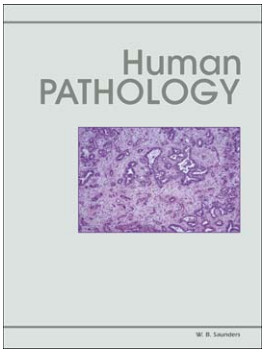

Sclerostin Expression in Skeletal Sarcomas

Jia Shen PhD, Carolyn A. Meyers BS, Swati Shrestha BS, Arun Singh MD, Greg LaChaud BS, Vi Nguyen BS, Greg Asatrian BS, Noah Federman MD, Fritz C. Eilber MD, Sarah M. Dry MD, Kang Ting DMD, DMedSci, Chia Soo MD, Aaron W. James MD

PII: S0046-8177(16)30168-X
DOI: doi: 10.1016/j.humpath.2016.07.016
Reference: YHUPA 3964

To appear in: *Human Pathology*

Received date: 6 April 2016
Revised date: 15 July 2016
Accepted date: 20 July 2016

Please cite this article as: Shen Jia, Meyers Carolyn A., Shrestha Swati, Singh Arun, LaChaud Greg, Nguyen Vi, Asatrian Greg, Federman Noah, Eilber Fritz C., Dry Sarah M., Ting Kang, Soo Chia, James Aaron W., Sclerostin Expression in Skeletal Sarcomas, *Human Pathology* (2016), doi: 10.1016/j.humpath.2016.07.016

Sclerostin Expression in Skeletal Sarcomas

Jia Shen, Ph.D.[a,b], Carolyn A. Meyers, B.S.[b], Swati Shrestha, B.S.[b], Arun Singh, M.D.[c], Greg LaChaud, B.S.[a,b], Vi Nguyen, B.S.[b], Greg Asatrian, B.S.[a,b], Noah Federman, M.D.[d], Fritz C. Eilber, M.D.[g], Sarah M. Dry, M.D.[b], Kang Ting, D.M.D., D.Med.Sci.[a], Chia Soo, M.D.[e,f], Aaron W. James, M.D.[b,f]

[a] Division of Growth and Development and Section of Orthodontics, School of Dentistry, 90095; [b] Department of Pathology and Laboratory Medicine, David Geffen School of Medicine, University of California, Los Angeles, 90095; [c] Division of Hematology/Oncology, David Geffen School of Medicine, University of California, Los Angeles, 90095; [d] Department of Pediatrics, David Geffen School of Medicine, University of California, Los Angeles, 90095; [e] Division of Plastic and Reconstructive Surgery, Department of Surgery, David Geffen School of Medicine, University of California, Los Angeles, 90095; [f] UCLA and Orthopaedic Hospital Department of Orthopaedic Surgery and the Orthopaedic Hospital Research Center, 90095; [g]Division of Surgical Oncology, University of California, Los Angeles, 90095

*Correspondence:

Aaron W. James, M.D.

Department of Pathology & Laboratory Medicine

University of California, Los Angeles, David Geffen School of Medicine

10833 Le Conte Ave., 13-145 CHS

Los Angeles, California 90095

Tel: (310) 206-6754

Fax: (310) 267-2058

Email: Awjames@mednet.ucla.edu

Running Title: SOST in skeletal tumors

Abstract

Sclerostin (SOST) is an extracellular Wnt signaling antagonist which negatively regulates bone mass. Despite this, the expression and function of SOST in skeletal tumors remains poorly described. Here, we first describe the immunohistochemical staining pattern of SOST across benign and malignant skeletal tumors with bone or cartilage matrix (n=68 primary tumors). Next, relative *SOST* expression was compared to markers of Wnt signaling activity and osteogenic differentiation across human osteosarcoma cell lines (n=7 cell lines examined). Results showed immunohistochemical detection of SOST in most bone-forming tumors (90.2%, 46/51) and all cartilage-forming tumors (100%, 17/17). Among osteosarcoma (OS), variable intensity and distribution of SOST expression was observed, which highly correlated with the presence and degree of neoplastic bone. Patchy SOST expression was observed in cartilage-forming tumors, which did not distinguish between benign and malignant tumors or correlate with regional morphologic characteristics. Finally, *SOST* expression varied widely between OS cell lines, with >97 fold variation. Among OS cell lines, *SOST* expression positively correlated with the marker of osteogenic differentiation *Alkaline Phosphatase (ALP)*, and did not correlate well with markers of Wnt/β-catenin signaling activity. In summary, Sclerostin is frequently expressed in skeletal bone- and cartilage-forming tumors. The strong spatial correlation with bone formation and the *in vitro* expression patterns are in line with the known functions of SOST in non-neoplastic bone, as a feedback inhibitor on osteogenic differentiation. With anti-SOST as a potential therapy for osteoporosis in the near future, its basic biologic and phenotypic consequences in skeletal tumors should not be overlooked.

Keywords: SOST; Wnt signaling; sarcoma; osteosarcoma; enchondroma; chondrosarcoma

1. Introduction

Sclerostin (SOST) is an extracellular Wnt signaling antagonist with high endogenous expression in osteocytes(1, 2). Human disorders of SOST expression and activity result in bone overgrowth in rare autosomal recessive syndromes, including sclerosteosis and Van Buchem disease. SOST is well described to negatively regulate osteogenesis and bone mass(1, 2), and targeted *Sost* deletion in mice results in a high BMD phenotype with increased bone strength(3). Consequently, significant interests exist in the use of anti-SOST neutralizing antibodies for the clinical entity of osteoporosis, such as romosozumab (AMG 785, Amgen Inc., Thousand Oaks, CA)(4-6) and blosozumab (LY2541546, Eli Lilly and Company, Indianapolis, IN). Preclinical studies have shown that anti-Sost antibodies inhibit bone loss in ovariectomy(7, 8), in the aged skeleton, and during fracture healing(9, 10). The expression and function of SOST in skeletal tumors remains poorly understood.

The importance of avoiding tumorigenesis cannot be overlooked in the field of osteoporotic therapies. This issue has growing importance with protein-based bone anabolism. For example, the main FDA approved recombinant protein for local bone formation is BMP2 (Bone Morphogenetic Protein 2). BMP ligands and BMP receptors are expressed in most osteosarcoma (OS) cell lines and OS subtypes. Moreover, although disagreement in the literature exists, the presence of BMP signaling in OS may impart a worse prognosis(11). On the cellular level, BMP signaling appears to mediate pro-migratory effects in both OS and chondrosarcoma (CS) cell types. Likewise, Parathyroid Hormone (PTH) is the main FDA approved anabolic agent in the treatment of osteoporosis. Unfortunately, the clinical duration of use for PTH is limited to 24 months, owing to the potential risk of osteosarcomagenesis (as documented in rat studies)(12). Thus, currently approved agents for bone anabolism are not without potential risks for skeletal sarcomagenesis.

There is to date little known regarding SOST expression and function in skeletal sarcomas. Several pieces of data suggest that SOST has diverse roles in epithelial malignancies, including breast carcinoma, prostate carcinoma, thyroid carcinoma, and renal cell carcinoma. In general, studies have demonstrated that overexpression of numerous Wnt components in OS (including Wnt ligands, Frizzled,

and LRP receptors), highlighting the implications of aberrant Wnt/β-catenin signaling in OS progression(13, 14) . In contrast, Wnt antagonists are generally reduced in OS. For example, *WIF-1* mRNA expression was significantly decreased in numerous OS cell lines in comparison to normal human osteoblasts, attributed to WIF-1 promoter hypermethylation(15). Investigators found that WIF-1 downregulates the expression of MMP-9 and 14, thereby preventing the invasion and mobility of OS cells(15). Kansara *et al.* further confirmed that WIF-1 is epigenetically silenced in human OS, and targeted disruption of WIF-1 accelerates OS formation in mice(16). Likewise, expression of other Wnt/β-catenin inhibitors, such as FrzB/sFRP3, is consistently suppressed in OS(17). Conversely, in CS increased *DKK1* expression was recently observed to correlate with high Wnt signaling activity and a poor prognosis(18). Despite this, the expression and function of SOST in skeletal tumors is poorly understood. Here, we provide a comprehensive description of SOST expression in skeletal bone- and cartilage-forming tumors.

2. Materials and Methods

2.1 Antibodies and reagents

Primary antibodies used in this study were anti-SOST (ab75914, Abcam). All other reagents were purchased from Dako unless otherwise specified.

2.2 Tissue Procurement

Tumors were retrospectively collected from biopsy and resection specimens at the University of California, Los Angeles under IRB# 13-897. Each tumor was re-examined by two blinded bone tissue pathologists to ensure accuracy of original diagnosis. When appropriate, radiographs were also examined to confirm concordance with the pathologic diagnosis. Demographic features and specific tumor measurements were recorded, including patient age, gender, anatomic location, tumor size, and history of neoadjuvant therapy (**Supplementary Table 1**). When available, undecalcified samples were chosen for

immunohistochemical staining. 52.8% of samples were decalcified (28/53 samples), including 20/36 benign and malignant bone-forming tumors and 8/17 benign and malignant cartilage-forming tumors.

2.3 Histological and immunohistochemical analyses

Five-micron-thick paraffin sections of bone and cartilage tumors were stained with haematoxylin and eosin (H&E). Using H&E sections, histomorphologic assessments were made to confirm tumor type and to determine characteristics of different regions within each section. Additional sections were analyzed by indirect immunohistochemistry. Briefly, unstained sections were deparaffinized in xylene and a series of graded ethanol solutions, and rehydrated using phosphate buffered solution. The slides were incubated in 3% hydrogen peroxide for 20 min at room temperature to block endogenous peroxidase activity. 0.125% trypsin induced epitope retrieval was performed for 20 min at room temperature, using the "Digest-All 2" system (Cat 00-3008, Invitrogen, Grand Island, NY). Slides were then incubated with the primary antibody for 1 hr at 37º Celsius and 4º Celsius overnight. The anti-SOST primary antibody was used at a dilution of 1:50. After incubation with the primary antibody, slides were incubated with an appropriate biotinylated secondary antibodies (Dako) for 1 hr at room temperature, used at 1:200 dilution.

Positive immunoreactivity was detected following ABC complex (PK-6100, Vectastain Elite ABC Kit, Vector Laboratories Inc., Burlingame, CA) incubation and development with AEC chromagen (K346911-2, Dako). Negative controls for each antibody consisted of incubation with secondary antibody in the absence of primary antibody. Sections of non-neoplastic human cortical bone were used in each instance as a positive staining control. Sections were counterstained in Modified Mayers Hematoxylin (Thermo Scientific, Waltham, MA) for 30 seconds, and placed under running water for 5 min. Slides were mounted using aqueous mounting medium (Dako). Photomicrographs were acquired using Olympus BX51 (UPLanFL, Olympus).

Intensity and distribution of immunohistochemical stainings were determined by three blinded observers. The intensity of staining was estimated using a 3 point scale, with '0' indicating no staining, '1+' indicating predominantly faint/barely perceptible cytoplasmic staining within any percentage of tumor cells, '2+' indicating predominantly weak/moderate cytoplasmic staining within any percentage of tumor cells, and '3+' indicating strong/intense cytoplasmic staining within any percentage of tumor cells. Discrepancies in semi-quantification of intensity of staining between observers were found in less than 10% of samples. In this case, the intensity of stain was determined by consensus re-review of the slides by all three observers. Distribution of staining was determined on a continuous 0%-100% scale, estimating the percentage of tumor cells with SOST immunoreactivity in 5% increments.

2.4 Regular PCR and Quantitative RT-PCR

Cells were expanded in standard growth mediums according to cell type, including either (1) DMEM + 10% FBS (HOS, MNNG, 143B, KHOS312H, KHOS), (2) RPMI + 10% FBS (SJSA), or (3) McCoys medium + 20% FBS (G292). Quantitative real time PCR for *SOST*, Wnt signaling activity and bone specific markers was performed upon subconfluency using 6 well culture dishes. Primer sequences are shown in **Supplementary Table 2**. Methods for regular PCR and quantitative real time PCR are as previously described, performed in triplicate per RNA isolate(19). In addition, *SOST* and osteogenic marker expression was assayed at serial timepoints under osteogenic differentiation conditions (0, 3, 6, and 9 days). Osteogenic medium included basal medium supplemented with 50 μg/mL ascorbic acid and 3 mmol/L β-glycerophosphate. For RNA expression among primary tumors, samples were snap frozen in liquid nitrogen as soon as possible after surgical removal. Tissue homogenization and RNA extraction was performed as previously described(19).

2.5 Statistical analysis

Statistical analysis was performed using an appropriate Student's *t*-test when two groups of numerical values were being compared, as in the case of staining distribution. A Fisher's exact test was performed to determine statistical significance of contingency tables, as in the case of staining intensity. In general, a p-value less than 0.05 was considered statistically significant.

3. Results

3.1 SOST expression in benign bone tumors

All cases of osteoid osteoma and osteoblastoma demonstrated characteristic anastomosing trabeculae of woven bone, with a single layer of activated osteoblasts and variable multi-nucleated osteoclasts (**Fig. 1**). Weak to intermediate staining intensity for SOST was apparent across all samples. Immunoreactivity was generally in a cytosolic distribution, and was observed in a diverse array of cell types within the tumor nidus including most commonly bone-lining osteoblasts, bone-entombed osteocytes, multinucleated giant cells, as well as mononuclear cells within the stroma. Semi-quantification of SOST immunoreactivity in benign bone-forming tumors demonstrated intermediate to strong intensity of staining in all samples (2-3+) with the large minority of tumor cells showing immunoreactivity (on average 47.0% and 48.0% of tumors cells within osteoid osteoma and osteoblastoma, respectively) (**Table 1**).

3.2 SOST expression in conventional osteosarcoma

Next, SOST immunoreactivity was examined in osteoblastic osteosarcoma (OS) specimens. Demographic information can be found in **Supplementary Table 1**. A wide array of tissue types were examined, including initial biopsies, primary resection, and metastatectomy specimens. 46% of tumors (12/26) were from biopsy or resection samples with no history of chemotherapy or radiation. Results showed that among osteoblastic OS, SOST expression highly correlated with bone matrix expression

(**Fig. 2A-D**). Across samples, we observed high SOST immunoreactivity in those osteoblastic cells lining and immediately adjacent to bone deposition. This was particularly apparent in samples with chemotherapy induced 'differentiation.' Regular PCR confirmed expression of *SOST* among osteoblastic OS samples on the gene level (**Supplementary Fig. 1**). Chondroblastic OS samples showed a similar phenomenon with SOST immunoreactivity in and around areas of endochondral ossification (**Fig. 2E-H**). SOST immunostaining was particularly seen in areas of mineralized cartilage and bone (**Fig. 2E,F**), but was also in present in areas without mineralization (**Fig. 2G,H**). Finally, subtypes of conventional OS with minimal bone deposition were examined, including fibroblastic OS and giant cell rich OS. These subtypes with minimal bone matrix showed infrequent SOST immunoreactive cells (**Fig. 2I,J,** giant cell rich OS shown). In these samples with minimal neoplastic bone, sparse SOST expression was present in osteoblastic cells in and around the bone matrix. Semi-quantification of SOST immunohistochemical staining was variable and reflected the range of bone production among OS samples (**Table 1**). The intensity of staining ranged from weak to strong (1-3+) with on average approximately 42.4% (±31%) of tumor cells demonstrating positive staining (n=41 specimens). No difference in staining intensity or distribution was seen when comparing OS samples to benign bone-forming tumors (p=0.19 and 0.54, respectively). Osteoblastic OS and chondroblastic OS showed a similar pattern of SOST staining, with most showing moderate to strong intensity (2-3+) in the large minority of tumor cells (40.4% and 33.2% of tumor cells, respectively). Fibroblastic OS and giant cell rich OS showed focal staining that was weak to moderate in intensity (1-2+). Of note, only viable tumor was considered in semi-quantitative grading schemes.

To further document the relationship between neoplastic bone matrix and SOST immunohistochemical staining, serial random high magnification images from conventional OS were quantified both for the degree of SOST staining and amount of bone matrix (**Fig. 2K**). Briefly, total SOST immunoreactivity per 40x field and total bone matrix per 40x field were quantified using Adobe Photoshop, and each high

magnification image was placed on a scatterplot. Results confirmed a significant correlation between relative SOST immunostaining and bone matrix production (correlation coefficient, R^2=0.6788). In summary, conventional OS showed a reproducible immunohistochemical staining pattern for SOST, with the degree and localization of stain highly correlated with bone matrix production.

3.3 SOST expression in osteosarcoma subtypes

We next sought to examine SOST expression among distinct OS subtypes (including parosteal, periosteal, and telangiectatic OS). Examination of parosteal OS specimens revealed a characteristic dual lineage tumor with alternating zones of bony trabeculae and fibroblastic stroma (**Fig. 3A-F**). A relative abundance of SOST immunostaining was observed among parosteal OS samples. Staining of variable intensity was observed in a majority of parosteal tumor cells (1-3+ intensity, 61% of tumor cells). Notably, SOST expression was observed both in the spindle cell population of fibroblastic areas and also within osteocytes of neoplastic bone (**Fig. 3A-F**). Examination of periosteal OS revealed characteristic feather-like osteoid surrounded by zones of intermediate grade chondroblastic differentiation (**Supplementary Fig. 2**). Like conventional OS, SOST immunoreactivity was seen in areas of ossification (2+ staining intensity, *not shown*). Finally, telangiectatic osteosarcoma specimens were examined which demonstrated a characteristic appearance of highly atypical neoplastic cells in a background of blood, fibrin and sparse bone. Among telangiectatic OS specimens, SOST immunoreactivity was again noted in areas of ossification in the minority of cells (1-3+, 26% of tumor cells). Tumors without bone deposition showed no detectable SOST expression (**Fig. 3G,H**). In summary, like conventional OS, most OS variants demonstrate SOST immunoreactivity in and around areas of neoplastic bone. Parosteal OS is the notable exception to this observation, which showed significant SOST expression among both fibrous and osseous components.

3.4 SOST expression among OS cell lines

SOST expression was next assayed across OS cell lines (**Fig. 4**). Results showed a wide variation across OS cell lines (>97 fold variation) (**Fig. 4A**). Those high expressing *SOST* cell lines included SJSA, HOS and MNNG. Basal *SOST* expression did not appear to correlate well with known comparative growth rates, cellular morphology, or metastatic potential(20-26).

We next inquired as to whether *SOST* expression correlated with markers of canonical Wnt signaling or osteogenic differentiation among seven OS cell lines, as assessed by quantitative RT-PCR (**Fig. 4B-F**). We first inquired as to whether high *SOST* expression correlated with low Wnt/β-catenin signaling activity, as could be hypothesized from the known functions of SOST as an extracellular Wnt inhibitor (**Fig. 4B-D**). Markers of Wnt/β-catenin signaling used included *AXIN2*, *CYCLIN D*, and *CMYC* (**Fig. 4B-D**), with each dot on a scatter plot representing a different OS cell line. Overall, markers of Wnt/β-catenin signaling activity did not correlate well with *SOST* expression. A line of best fit for each gene correlation to SOST is shown (**Fig. 4B-D**). Correlation coefficients were close to zero for all comparisons (R^2 range: 0.04736-0.07395). Next, basal expression of markers of osteogenic differentiation was compared to *SOST* expression across OS cell lines (**Fig. 4E,F**). Of the genes assessed, *ALP* expression (*Alkaline phosphatase,* a marker of osteoblastic differentiation) showed a positive correlation with *SOST* expression, (R^2=0.46793). In contrast, *RUNX2* showed no correlation with *SOST* expression, (R^2=0.00255). In aggregate, only the marker of osteogenic differentiation *ALP* showed a correlation with *SOST* expression among OS cell lines.

Next, we assayed *SOST* expression during the osteogenic differentiation of OS cell lines (**Fig. 4G,H**). In general, *SOST* expression has been reported to increase overtime in osteoblastic cell culture. For this purpose, low *SOST* expressing cell lines (including KHOS312H and G292 lines) were examined under

standard osteogenic conditions from 0-9 days of differentiation. Results showed a significant and time dependent induction of *SOST* expression with osteogenic conditions across both cell lines examined. The absolute change in *SOST* expression varied widely (overall 19- and 13,045-fold upregulations for G292 and KHOS312H cells, respectively – a nearly 700 fold difference in absolute change). Next, changes in *SOST* expression overtime under differentiation conditions were compared to the osteogenic markers *RUNX2* and *OCN* (**Supplementary Tables 3,4**). For this purpose, relative *SOST* expression was normalized to either *RUNX2* or *OCN* expression overtime in osteogenic culture. Overall, the degree of increase in *SOST* expression was higher than the degree of increase in either osteogenic marker. This was observed in both KHOS312H and G292 cells (**Supplementary Tables 3,4**). Overall, *SOST* expression seemed to correlate with osteogenic gene expression during osteogenic differentiation conditions.

3.5 SOST expression in cartilage-forming tumors

Next, SOST expression was compared across benign and malignant cartilage forming tumors (**Fig. 5**). All tumors showed some degree of SOST immunoreactivity in the minority of tumor cells (17/17 samples, **Table 1**). SOST expression did not necessarily correlate with areas of mineralization or myxoid change in either enchondroma or chondrosarcoma. In enchondroma, SOST immunoreactivity was most often of moderate intensity (2+ in 4/5 tumors) and in the minority of tumor cells (21.0%, ±16.4%). In chondrosarcoma, SOST immunoreactivity was likewise most often of moderate intensity (2+, 58.35% of tumors). Chondrosarcoma cells showed a large and more variable distribution of SOST immunoreactivity than their benign counterparts (50.0%, ±27.3%). In summary, SOST expression is ubiquitous among both benign and malignant tumors with hyaline cartilage. No statistically significant difference in staining intensity or distribution was observed between benign and malignant cartilage-forming tumors ($p=0.76$ and $p=0.44$, respectively).

4. Discussion

In brief, the present study has identified several unique features of SOST in skeletal tumors. First, SOST expression is present to some degree across nearly all bone- and cartilage-forming skeletal tumors. Second, the distribution of SOST among OS tumors correlated highly with neoplastic bone deposition, while among CS specimens a correlation with any histopathologic features was not observed. *In vitro* studies among OS cell lines suggested a positive correlation of *SOST* with the osteogenic differentiation marker *Alkaline Phosphatase (ALP)*, while no significant correlation was observed between *SOST* expression and markers of Wnt signaling activity.

Our results have similarities and differences to the recently reported expression profiles of SOST by Inagaki *et al*. Like our study, Inagaki *et al.* described SOST expression across the majority of bone and cartilage tumors, including both benign and malignant tumors. Several findings in our study are in disagreement with their reports, including: (1) presence of SOST staining among bone-lining cells of osteoid osteoma and osteoblastoma, (2) presence of SOST staining in chondroblastic OS, (3) distinctive patterns of SOST expression in parosteal OS in both fibroblastic and osseous components, and (4) SOST staining among all cartilaginous tumors examined (including low and high grade chondrosarcoma) that did not necessarily correlate with mineralization. It should be noted that factors such as rarity of tumors, antibody selection, and variable tissue processing may well explain these discrepancies between our two studies.

The expression of SOST in OS and CS raises intriguing questions regarding its role in the basic function in skeletal sarcoma tumor biology. The role of other Wnt signaling antagonists has been explored in OS and CS, including WIF-1, SFRP3, and DKK1. In general, numerous Wnt signaling components have been described as upregulated among OS and CS tumors(13, 14, 27) (although this is not entirely agreed upon in the literature(28)), while Wnt antagonists such as WIF1 and SFRP3 are generally reduced(15-17). In contrast, DKK1 appears to be upregulated in OS, both locally and

systemically(29). In CS, DKK1 overexpression when combined with increased Wnt signaling activity portends a worse clinical outcome(18). Our data clearly localize SOST to OS cells with osteoblastic differentiation. This is not unlike its native expression in osteocytes, and a potential role for SOST in repressing bone formation in OS is a reasonable hypothesis given its distribution. In cartilaginous tumors, the role of SOST is less clear based on its patchy expression pattern, which in our hands did not correlate well with areas of mineralization or myxoid change. Importantly, simple detection of SOST in human cell lines and human skeletal tumors does not necessarily imply retained bioactivity. It is intriguing, however, to link the overproduction of SOST in OS tumors to the high incidence of osteoporosis among long term surviving OS patients(30,31). However, osteoporosis among this patient population is no doubt multifactorial, with contributing factors including exposure to chemotherapeutic agents, poor nutrition, and decreased physical activity. At this point, the potential link between SOST overproduction and osteoporosis among OS patients is a theoretical one.

Several limitations exist for broader extrapolation of the results from the present study. First, we rely on immunohistochemical based detection of SOST in human tumor samples, which is inherently a descriptive methodology. Moreover, clinical samples vary in their processing, with variable lengths of ischemic time, fixation time, and decalcification time. How these factors influence the SOST antigen is not yet known. Finally, expression profiles within cell lines and primary tumors represent an important step forward in understanding the potential role of SOST in skeletal pathophysiology, but is limited by its descriptive nature. Further studies to examine the prognostic importance of SOST expression, as well as the cellular consequences of SOST dysregulation, may shed light on these issues.

5. Concluding Remarks

The present study highlights the presence of SOST across benign and malignant bone- and cartilage-forming skeletal tumors. SOST strongly localizes to areas of osteoblastic differentiation and ossification.

6. Disclosure / Conflict of Interest

None.

7. Acknowledgments

The present work was supported by the UCLA Department of Pathology and Laboratory Medicine, the Translational Research Fund, the UCLA Daljit S. and Elaine Sarkaria Fellowship award, the Orthopaedic Research and Education Foundation with funding provided by the Musculoskeletal Transplant Foundation, and NIH/NIAMS K08 AR068316-01. The authors thank the staff of UCLA Translational Pathology Core Laboratory, Dr. N. Bernthal, and A.S. James for their excellent technical assistance.

8. References

1. Martin TJ. Bone biology and anabolic therapies for bone: current status and future prospects. J Bone Metab 2014; 21, 8-20.
2. Hoeppner LH, Secreto FJ, Westendorf JJ. Wnt signaling as a therapeutic target for bone diseases. Expert Opin Ther Targets 2009; 13, 485-496.
3. Li X, Ominsky MS, Niu QT, Sun N, Daugherty B, D'Agostin D, Kurahara C, Gao Y, Cao J, Gong J, Asuncion F, Barrero M, Warmington K, Dwyer D, Stolina M, Morony S, Sarosi I, Kostenuik PJ, Lacey DL, Simonet WS, Ke HZ, Paszty C. Targeted deletion of the sclerostin gene in mice results in increased bone formation and bone strength. J Bone Miner Res 2008; 23, 860-869.
4. McClung MR, Grauer A, Boonen S, Bolognese MA, Brown JP, Diez-Perez A, Langdahl BL, Reginster JY, Zanchetta JR, Wasserman SM, Katz L, Maddox J, Yang YC, Libanati C, Bone HG. Romosozumab in postmenopausal women with low bone mineral density. N Engl J Med 2014; 370, 412-420.
5. Costa AG, Bilezikian JP, Lewiecki EM. Update on romosozumab : a humanized monoclonal antibody to sclerostin. Expert Opin Biol Ther 2014; 14, 697-707.
6. Minisola S. Romosozumab: from basic to clinical aspects. Expert Opin Biol Ther 2014; 14, 1225-1228.
7. Ominsky MS, Niu QT, Li C, Li X, Ke HZ. Tissue-level mechanisms responsible for the increase in bone formation and bone volume by sclerostin antibody. J Bone Miner Res 2014; 29, 1424-1430.
8. Stolina M, Dwyer D, Niu QT, Villasenor KS, Kurimoto P, Grisanti M, Han CY, Liu M, Li X, Ominsky MS, Ke HZ, Kostenuik PJ. Temporal changes in systemic and local expression of bone turnover markers during six months of sclerostin antibody administration to ovariectomized rats. Bone 2014; 67, 305-313.

9. Yao Q, Ni J, Hou Y, Ding L, Zhang L, Jiang H. Expression of sclerostin scFv and the effect of sclerostin scFv on healing of osteoporotic femur fracture in rats. Cell Biochem Biophys 2014; 69, 229-235.
10. Alaee F, Virk MS, Tang H, Sugiyama O, Adams DJ, Stolina M, Dwyer D, Ominsky MS, Ke HZ, Lieberman JR. Evaluation of the effects of systemic treatment with a sclerostin neutralizing antibody on bone repair in a rat femoral defect model. J Orthop Res 2014; 32, 197-203.
11. Yoshikawa H, Takaoka K, Masuhara K, Ono K, Sakamoto Y. Prognostic significance of bone morphogenetic activity in osteosarcoma tissue. Cancer 1988; 61, 569-573.
12. Vahle JL, Sato M, Long GG, Young JK, Francis PC, Engelhardt JA, Westmore MS, Linda Y, Nold JB. Skeletal changes in rats given daily subcutaneous injections of recombinant human parathyroid hormone (1-34) for 2 years and relevance to human safety. Toxicologic pathology 2002; 30, 312-321.
13. Chen K, Fallen S, Abaan HO, Hayran M, Gonzalez C, Wodajo F, MacDonald T, Toretsky JA, Uren A. Wnt10b induces chemotaxis of osteosarcoma and correlates with reduced survival. Pediatric blood & cancer 2008; 51, 349-355.
14. Hoang BH, Kubo T, Healey JH, Sowers R, Mazza B, Yang R, Huvos AG, Meyers PA, Gorlick R. Expression of LDL receptor-related protein 5 (LRP5) as a novel marker for disease progression in high-grade osteosarcoma. Int J Cancer 2004; 109, 106-111.
15. Rubin EM, Guo Y, Tu K, Xie J, Zi X, Hoang BH. Wnt inhibitory factor 1 decreases tumorigenesis and metastasis in osteosarcoma. Molecular cancer therapeutics 2010; 9, 731-741.
16. Kansara M, Tsang M, Kodjabachian L, Sims NA, Trivett MK, Ehrich M, Dobrovic A, Slavin J, Choong PF, Simmons PJ, Dawid IB, Thomas DM. Wnt inhibitory factor 1 is epigenetically silenced in human osteosarcoma, and targeted disruption accelerates osteosarcomagenesis in mice. J Clin Invest 2009; 119, 837-851.
17. Mandal D, Srivastava A, Mahlum E, Desai D, Maran A, Yaszemski M, Jalal SM, Gitelis S, Bertoni F, Damron T, Irwin R, O'Connor M, Schwartz H, Bolander ME, Sarkar G. Severe suppression of Frzb/sFRP3 transcription in osteogenic sarcoma. Gene 2007; 386, 131-138.
18. Chen C, Zhou H, Zhang X, Ma X, Liu Z, Liu X. Elevated levels of Dickkopf-1 are associated with beta-catenin accumulation and poor prognosis in patients with chondrosarcoma. PLoS One 2014; 9, e105414.
19. Shen J, James AW, Chung J, Lee K, Zhang JB, Ho S, Lee KS, Kim TM, Niimi T, Kuroda S, Ting K, Soo C. NELL-1 promotes cell adhesion and differentiation via Integrinbeta1. Journal of cellular biochemistry 2012; 113, 3620-3628.
20. Bruserud O, Tronstad KJ, Berge R. In vitro culture of human osteosarcoma cell lines: a comparison of functional characteristics for cell lines cultured in medium without and with fetal calf serum. J Cancer Res Clin Oncol 2005; 131, 377-384.
21. Lauvrak SU, Munthe E, Kresse SH, Stratford EW, Namlos HM, Meza-Zepeda LA, Myklebost O. Functional characterisation of osteosarcoma cell lines and identification of mRNAs and miRNAs associated with aggressive cancer phenotypes. Br J Cancer 2013; 109, 2228-2236.
22. Jian Y, Chen C, Li B, Tian X. Delocalized Claudin-1 promotes metastasis of human osteosarcoma cells. Biochem Biophys Res Commun 2015; 466, 356-361.
23. Gorska M, Krzywiec PB, Kuban-Jankowska A, Zmijewski M, Wozniak M, Wierzbicka J, Piotrowska A, Siwicka K. Growth Inhibition of Osteosarcoma Cell Lines in 3D Cultures: Role of Nitrosative and Oxidative Stress. Anticancer Res 2016; 36, 221-229.
24. Mu X, Isaac C, Greco N, Huard J, Weiss K. Notch Signaling is Associated with ALDH Activity and an Aggressive Metastatic Phenotype in Murine Osteosarcoma Cells. Front Oncol 2013; 3, 143.
25. Ren L, Mendoza A, Zhu J, Briggs JW, Halsey C, Hong ES, Burkett SS, Morrow J, Lizardo MM, Osborne T, Li SQ, Luu HH, Meltzer P, Khanna C. Characterization of the metastatic phenotype of a panel of established osteosarcoma cells. Oncotarget 2015; 6, 29469-29481.
26. Endo-Munoz L, Cai N, Cumming A, Macklin R, Merida de Long L, Topkas E, Mukhopadhyay P, Hill M, Saunders NA. Progression of Osteosarcoma from a Non-Metastatic to a Metastatic Phenotype Is

Causally Associated with Activation of an Autocrine and Paracrine uPA Axis. PLoS One 2015; 10, e0133592.
27. Chen C, Zhao M, Tian A, Zhang X, Yao Z, Ma X. Aberrant activation of Wnt/beta-catenin signaling drives proliferation of bone sarcoma cells. Oncotarget 2015; 6, 17570-17583.
28. Cai Y, Mohseny AB, Karperien M, Hogendoorn PC, Zhou G, Cleton-Jansen AM. Inactive Wnt/beta-catenin pathway in conventional high-grade osteosarcoma. J Pathol 2010; 220, 24-33.
29. Lee N, Smolarz AJ, Olson S, David O, Reiser J, Kutner R, Daw NC, Prockop DJ, Horwitz EM, Gregory CA. A potential role for Dkk-1 in the pathogenesis of osteosarcoma predicts novel diagnostic and treatment strategies. Br J Cancer 2007; 97, 1552-1559.

30. Holzer G, Krepler P, Koschat MA, Grampp S, Dominkus M, Kotz R. Bone mineral density in long-term survivors of highly malignant osteosarcoma. J Bone Joint Surg Br 2003; 85, 2, 231-7.

31. Lim JS, Kim DH, Lee JA, Kim DH, Cho J, Cho WH, Lee SY, Jeon DG. Young age at diagnosis, male sex, and decreased lean mass are risk factors of osteoporosis in long-term survivors of osteosarcoma. J Pediatr Hematol Oncol 2013; 35, 1, 54-60.

9. Figure Legends

Figure 1: SOST expression in benign bone-forming tumors. **(A-D)** H&E appearance of osteoblastoma and osteoid osteoma. **(E-H)** SOST immunohistochemical staining in osteoblastoma and osteoid osteoma. Scale bar: 100 μm.

Figure 2: SOST expression in conventional osteosarcoma (OS). **(A-D)** Appearance of H&E staining and SOST immunohistochemical staining in representative osteoblastic OS tumors. **(E-H)** Appearance of H&E staining and SOST immunohistochemical staining in representative chondroblastic OS tumors. **(I,J)** Appearance of H&E staining and SOST immunohistochemical staining in giant cell rich OS. Scale bar: 100 μm. **(K)** Relative SOST expression as a function of relative bone matrix in conventional OS. Individual random 40x fields are represented as a single blue dot. The y-axis demonstrates relative bone matrix abundance in comparison to relative SOST immunohistochemical staining on the x-axis. A line of best fit is shown.

Figure 3: SOST expression in osteosarcoma variants. Appearance of routine H&E staining and SOST immunohistochemical staining in **(A-F)** parosteal OS, and **(G,H)** telangiectatic OS. Scale bar: 100 μm.

Figure 4: Expression and correlation of *Sclerostin (SOST)* expression to gene markers of Wnt signaling activity and osteogenic differentiation across osteosarcoma (OS) cell lines, assessed by qRT-PCR. **(A)** Relative *SOST* expression across OS cell lines. N=3 replicates per group. Error bars represent one standard deviation. **(B)** Correlation of *SOST* expression to *AXIN2* expression. In scatterplots, each dot represents an OS cell line. The line of best fit is shown. **(C)** Correlation of *SOST* expression to *CYCLIND* expression. **(C)** Correlation of *SOST* expression to *CMYC* expression. **(E)** Correlation of *SOST* expression to *ALP (Alkaline phosphatase)* expression. **(F)** Correlation of *SOST* expression to *RUNX2 (Runt related transcription factor 2)* expression. N=3 replicates per group. **(G,H)** Expression of *Sclerostin (SOST)* during osteosarcoma (OS) cell osteogenic differentiation, assessed by qRT-PCR. **(G)** Relative *SOST* expression among KHOS312H cells (days 0-9 of differentiation). **(H)** Relative *SOST* expression among G292 cells (days 0-9 of differentiation). All data is normalized to housekeeping gene expression (*ACTB*).

Figure 5: SOST expression in cartilaginous tumors. **(A,B)** Appearance of H&E staining and SOST immunohistochemical staining in enchondroma. **(C-H)** Appearance of H&E staining and SOST immunohistochemical staining in among chondrosarcoma (CS) tumors, including **(C,D)** grade I, **(E,F)** grade II, and **(G,H)** grade III. Scale bar: 100 μm.

10. Tables

Table 1: Semi-quantitative assessment of Sclerostin immunohistochemistry, by tumor subtype.

	Staining Intensity (% of cases stained)	***Staining Distribution***			
Tumor Type (n)	***0***	***1+***	***2+***	***3+***	***Mean % of cells stained (±SD)***
Osteoid Osteoma (5)	-	-	3/5 (60%)	2/5 (40%)	**47.0% (±17.2%)**
Osteoblastoma (5)	-	-	4/5 (80%)	1/5 (20%)	**48.0% (±25.9%)**
Osteosarcoma (41)	**5/41 (12.2%)**	**8/41 (19.5%)**	**15/41 (36.6%)**	**13/41 (31.7%)**	**42.4% (±31.0%)**
Osteoblastic	4/22(18%)	2/22 (9%)	8/22 (36%)	8/22 (36%)	40.4%
Chondroblastic	2/14 (14%)	2/14 (14%)	6/14 (43%)	4/14 (29%)	33.2%
Fibroblastic	-	-	1/1(100%)	-	-
Giant Cell Rich	-	2/2 (100%)	-	-	-
Parosteal	-	3/7 (43%)	3/7 (43%)	1/7 (14%)	61.0%
Periosteal	-	-	1/1 (100%)	-	-
Telangiectatic	1/5 (20%)	-	1/5 (20%)	3/5 (60%)	26.0%
Enchondroma (5)	-	1/5 (20%)	4/5 (80%)	-	**21.0% (±16.4%)**
Chondrosarcoma (12)	-	2/12 (16.7%)	7/12 (58.3%)	3/12 (25.0%)	**50.0% (±27.3%)**
Grade 1	-	1/5 (20%)	3/5 (60%)	2/5 (40%)	61.0%
Grade 2	-	2/5 (40%)	3/5 (60%)	-	35.0%
Grade 3	-	-	1/2 (50%)	1/2 (50%)	55.0%

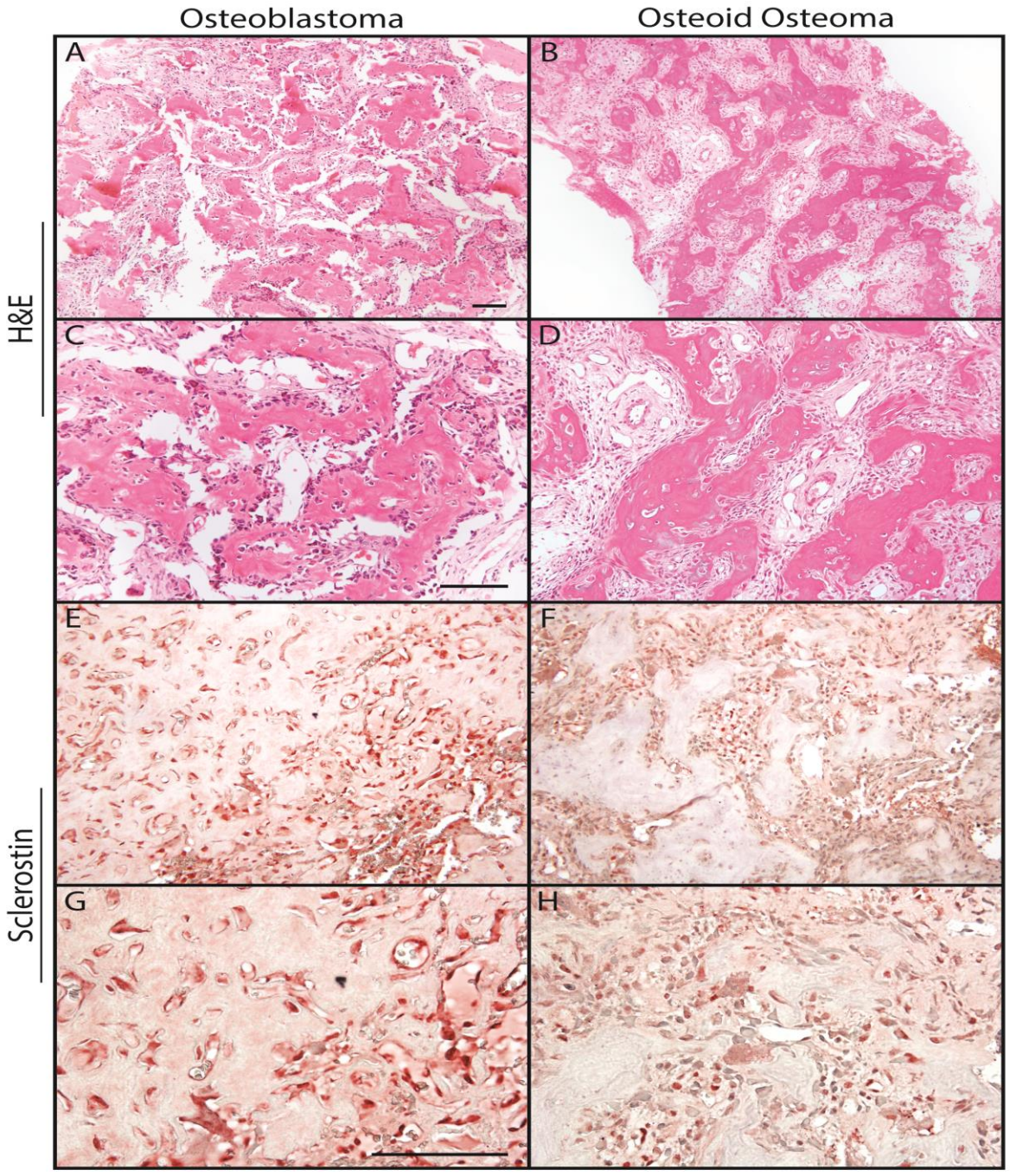

Figure 1

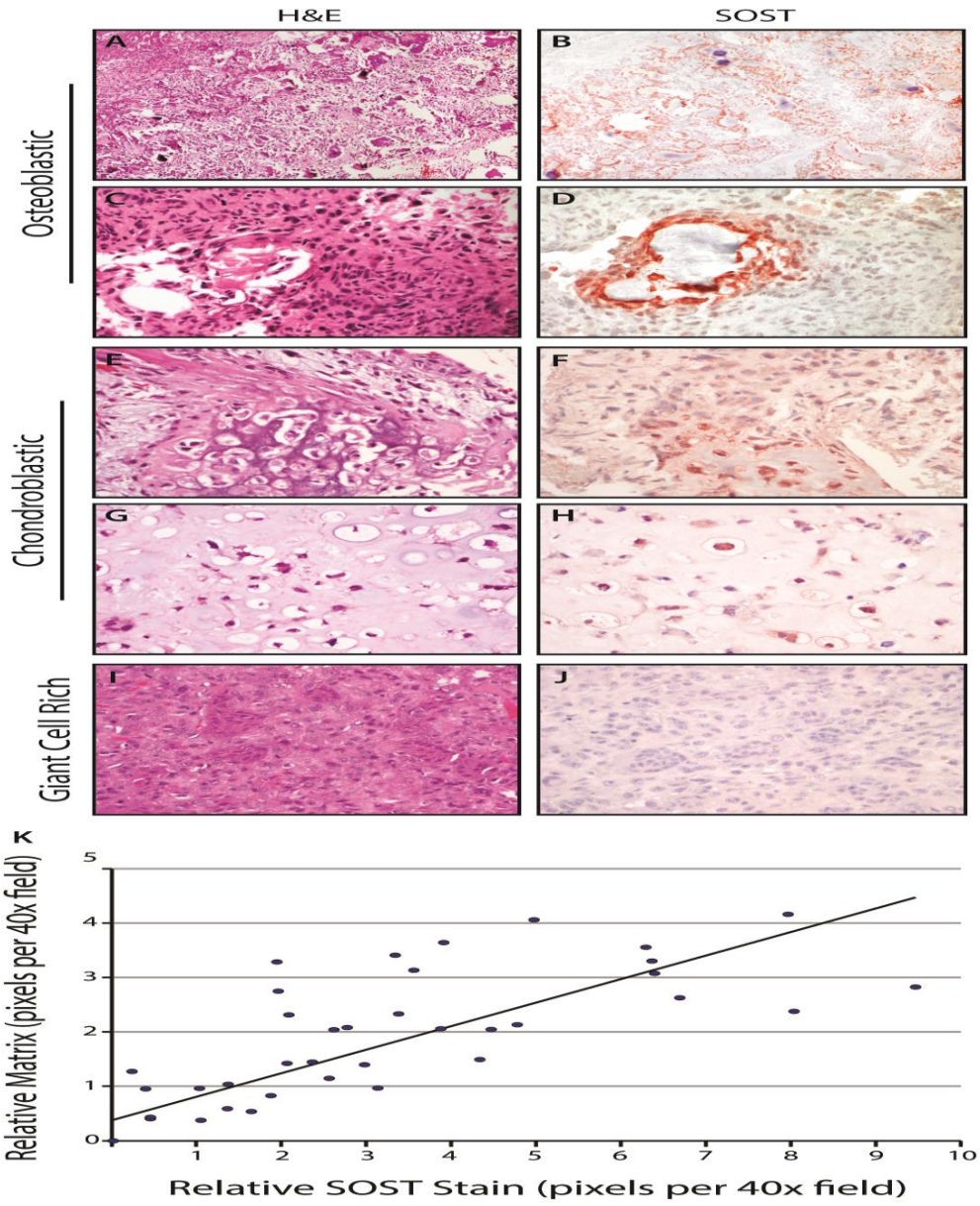

Figure 2

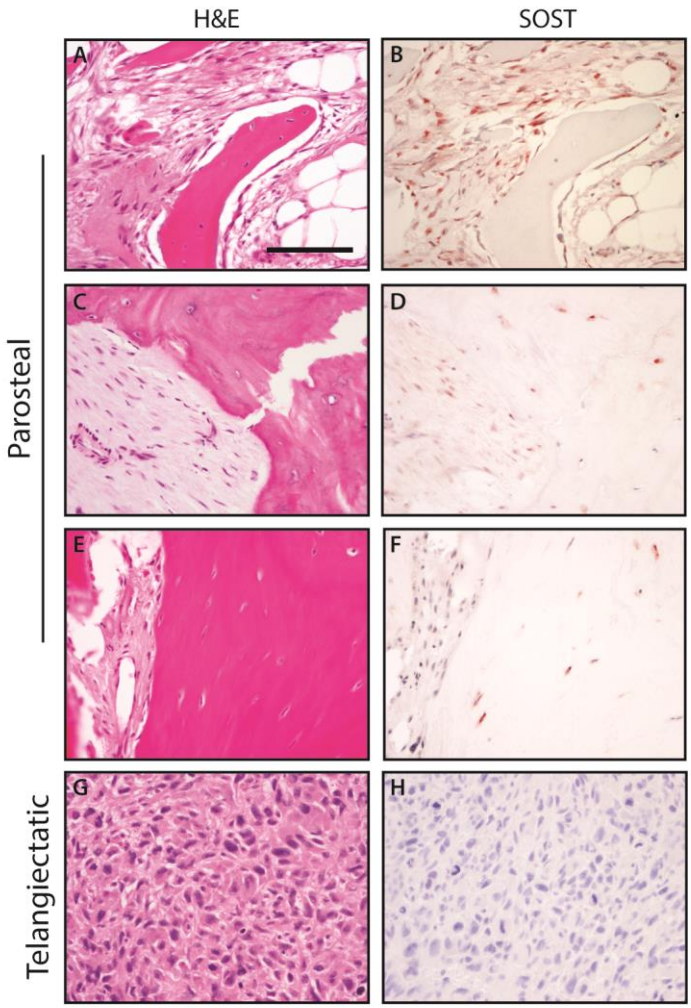

Figure 3

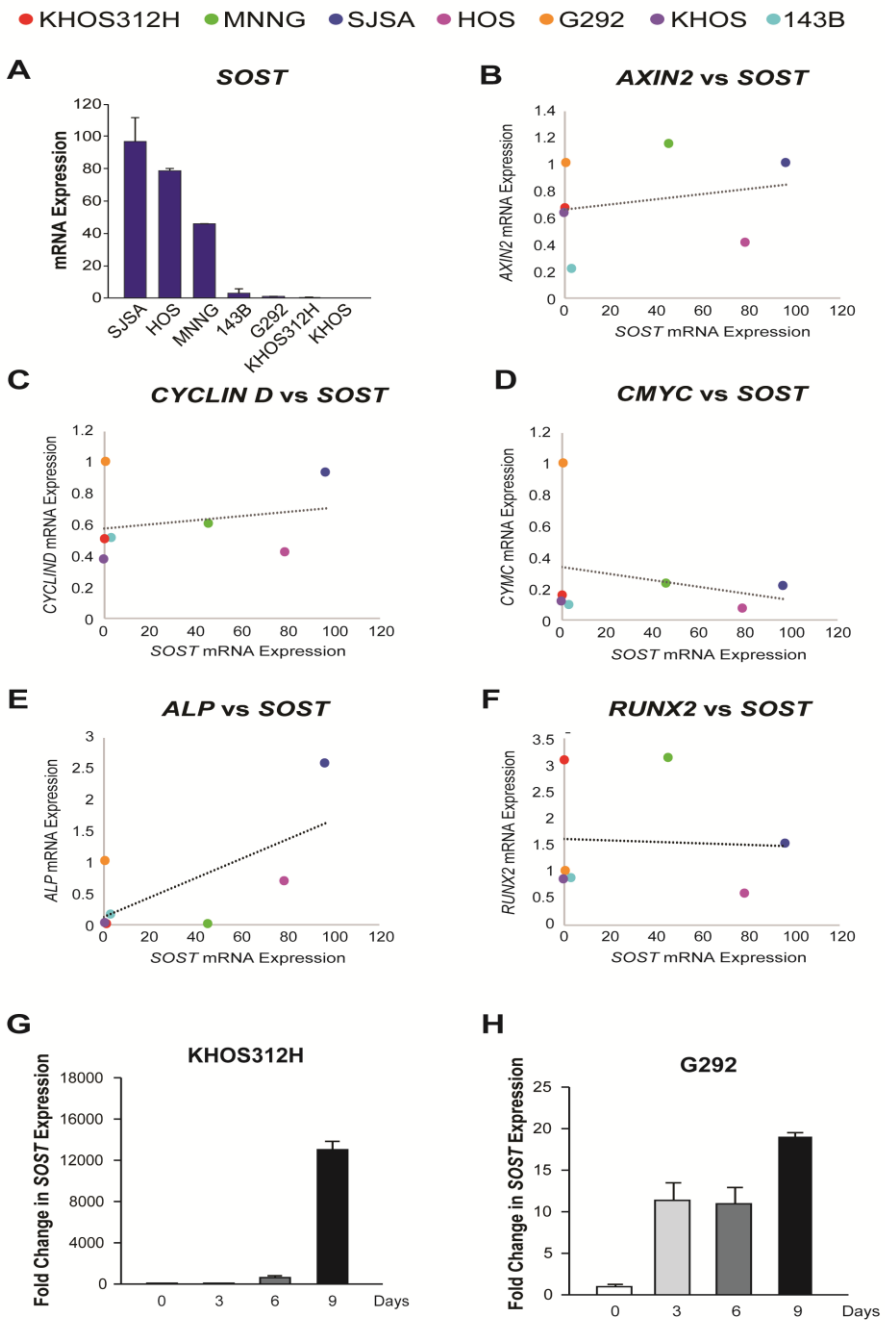

Figure 4

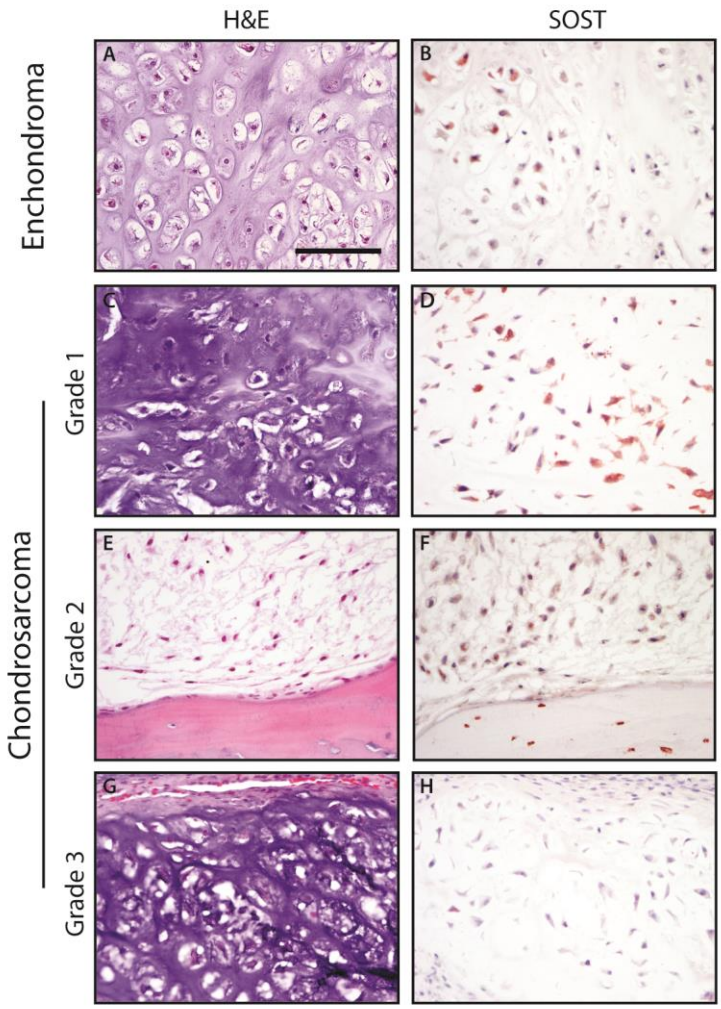

Figure 5